Detonation Output Properties of D-shape Structure

Ji-Feng Wei*, Chao Zhang, and Shu-Shan Wang

*State Key Laboratory of Explosion Science and Technology,
Beijing Institute of Technology, Beijing-100 081, China*
E-mail: weijifeng@bit.edu.cn

ABSTRACT

The detonation wave propagation and output properties have been analyzed for D-shape structure. Four initiation modes were designed to compare wavefront profiles and output pressure distribution. Simulation results show that three-array-nine-point initiation mode (Mode-III) brings about the most match-up wave front for D-shape structure. Detonation output properties have great influence on fragment ejection velocity and distribution density. The statistical results reveal that fragment parameters of Mode-III are the largest. Compared with Mode-III, the kinetic energies of other three modes decrease by 31.6 per cent, 19.6 per cent, 4.5 per cent, respectively. The computational values and normal curve of fragments distribution are obtained. From these analyses, it can be concluded that initiation mode has great influence on output parameters of fragments. With the optimal initiation Mode-III, ideal hitting angle should be within the range of -10° to 10°, the probability of distribution density would be close to 70 per cent.

Keywords: Detonation wave, initiation modes, wavefront profile, distribution density, numerical simulation

NOMENCLATURE

P_{CJ}	Detonation C-J pressure
D_{CJ}	Detonation velocity
A	Parameter of JWL equation
B	Parameter of JWL equation
R_1	Parameter of JWL equation
R_2	Parameter of JWL equation
E	Young's modulus

Greek symbols

ξ	Intersection angle
ρ	Material density
ω	Parameter of JWL equation
v	Poisson's ratio
σ	Material yield stress
β	Hardening parameter

Subscripts

CJ	*Chapman-Jouguet*

1. INTRODUCTION

Since the first recognition of detonation phenomenon in the last century, the propagation rule of detonation wave had intrigued great concern. As one of typical research issues, the behaviour and control of detonation wave propagation after interactions such as regular reflection and Mach reflection[1-3] had been widely studied. In these studies, the detonation wave could be affected by the diameter and curvature of charge under certain conditions[4-6]. Numerical simulation was a strong tool for the investigation of detonation wave structure and dynamics since the first three-dimensional wave was simulated by Williams[7], *et al*. By means of designing three kinds of shock configurations, Teng[8] studied the induction zone structures of oblique detonation waves with different Mach numbers. Zhang[9] designed a double-layer cylindrical high explosives configuration, where regular and irregular reflections of detonation waves were observed in computational program. At the collision point of Mach reflection, the maximum pressure can be upto 4-time of Chapman-Jouguet pressure. Wei[10] investigated detonation wave propagation of a D-shape confined structure which was controlled by three initiation points.

In fact, detonation wavefront is mainly controlled by initiation position and initiation number for a certain confined structure. Multi-point initiation is a well-known method to achieve a favourable wave[11-12]. In virtue of interactions of detonation waves, an expected wavefront appears. However, wavefront configuration would be quite complicated as the result of wave collisions and convergences. Compared with experiment, detonation wave propagation and ejection process can be observed clearly by numerical simulation[13,14].

D-shape structure is a better scheme to achieve directional dispersal of fragments. The purpose of research was to study the influence of detonation configuration with multi-point initiation on detonation output property. Four initiation modes were designed to investigate the evolution processes of detonation wavefronts by numerical simulation. The wave collisions and wave convergences were observed in three-dimensional wave configuration. At the same time, wavefront profiles and their pressure distributions are described in detail. Ejection results of fragments, such as ejection angle, fragment density, kinetic energy in hit angle, are calculated and compared. Based on these studies, the optimal initiation mode is obtained.

2. PHYSICAL STRUCTURE AND INITIATION MODES

2.1 Physical Structure

Usually the shape of confined shell for charge is cylindrical, and the fragments are symmetrically arranged along the cylinder circumference. However, D-shape geometric configuration has compressed explosive charge on one side, while the fragments are laid out on another side. This premade structure will lead a higher density fragment cloud to explode toward the target, which can not only increase the efficiency of explosive charge, but enhances damage probability to targets. D-shape structure is symmetric about the centreline, the larger curvature side is metallic case and the smaller curvature side is double-row spherical fragments. The condensed high energy explosive is filled in the body case. The cross section of D-shape structure is shown in Fig. 1.
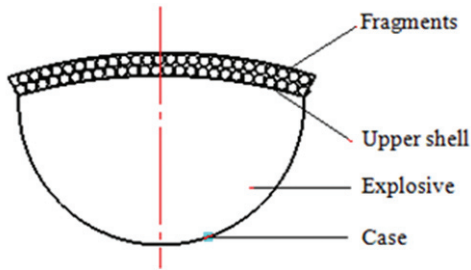
Figure 1. Cross section of D-shape structure.

2.2 Initiation Modes Design

To drive fragments in main ejection direction effectively, a match-up wave is needed. According to the design of structure, a match-up wave herein means that the final detonation wave shape needs to fit upper shell profile well. So, the design of initiation mode would be particularly important. That is because the oblique collisions of detonation waves can make the wave shape relatively flat if synchronous multi-point initiation mode is used. It not only make the fragments produce higher ejection velocity, but also makes fragments more concentrative. Namely, increasing synchronous detonation points can improve hitting ability.

Considering actual application of initiation mode, four initiation schemes were designed for D-shape structure. Side single initiation point (Mode-I), side three initiation points (Mode-II), side three-array-nine-point initiation mode (Mode-III and Mode-IV) are presented in Fig. 2. In Mode-I, the initiation point is placed in the centre of the curved surface. Three points are located on the middle cross section side surface in Mode-II. The three points in each array of Mode-III are placed in quartered point of generatrix. For Mode-IV,
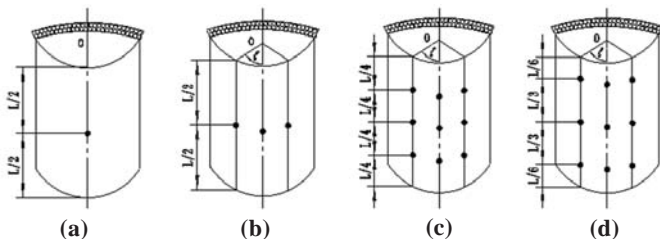
Figure 2. Four initiation modes: (a) Mode-I, (b) Mode-II, (c) Mode-III, and (d) Mode-IV.

initiation points are middle point of generatrix, two points of L/3 to middle point in axial distance. According to previous studies, when intersection angle ξ is set to 19°, the kill kinetic energy of fragments can be improved[10].

3. NUMERICAL SIMULATION MODEL

3.1 Numerical Model

The three-dimensional finite element model is made up of five parts including fragments, explosive, case, upper shell and lid, which is calculated by LS-DYNA code. Lagrange method can trace the boundaries of materials and display the whole drive process from explosive initiation to fragment dispersion. So explosive, case, upper shell, lid, and fragments are all established with Lagrangian meshes. Sliding contact algorithm is used for the contact between explosive and upper shell, while surface-to-surface contact algorithm is applied between upper shell and fragments. Three-dimensional finite element model is shown in Fig. 3.

There are two rows of fragments along the upper shell, the inner one has 34 fragments and the outer one has 33 fragments. A total of 1206 fragments, 18 layers are arranged along the axial direction.
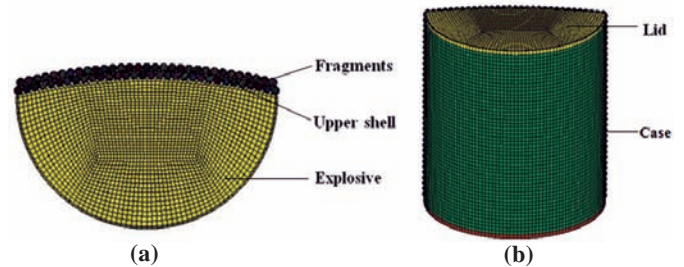
Figure 3. Three-dimensional finite element model for (a) section view and (b) back view.

3.2 Material Model and Parameters

Comp B charge is used for explosive, meanwhile the MAT_HIGH_EXPLOSIVE_BURN material model and JWL equation of state are adopted[15]. JWL can accurately describe the characteristics of pressure, volume and energy of detonation product in the driven process of detonation.

$$P = A\left(1 - \frac{\omega}{R_1 V}\right)e^{-R_1 V} + B\left(1 - \frac{\omega}{R_2 V}\right)e^{-R_2 V} + \frac{\omega E}{V} \qquad (1)$$

The detonation product pressure P is expressed as the function of relative volume V and internal energy E, A, B, R_1, R_2 and ω constants are determined by tests, the parameters of explosion property and the JWL equation of state are shown in Table 1.

The steel material is used for the shell and case, elastic and plastic deformation of the material is easily occurred under detonation, so MAT_PLASTIC_KINEMATIC material model is selected for the material model. The material of performed fragments is steel ball. MAT_RIGID material model is used to

Table 1. The detonation parameters of Comp B

ρ (kg/ m^3)	P_{CJ} (GPa)	D_{CJ} (m/s)	A (GPa)	B (GPa)	R_1	R_2	ω
1650	25.0	7800	1141.8	524.23	4.2	1.1	0.34

ensure integrity of fragments in the process of ejection[15]. The main material parameters are shown in Table 2.

Table 2. The parameters of steel material

Material model	ρ (kg/m³)	E (GPa)	v	σ (GPa)	β
Plastic_kinematic	7850	210	0.3	0.3	1.0
Rigid	7850	210	0.3	——	——

4. SIMULATION RESULTS AND ANALYSIS

4.1 Propagation Characteristics of Detonation Wave

On the basis of interaction mechanism of multi-point initiation of detonation wave, four kinds of detonation wave propagation characteristics are analysed in Figs 4-7. The propagation process of detonation wave is described respectively from initial initiation to wavefront reaching the upper shell. The figures of detonation wavefront are described by pressure contour.

Single detonation wave propagates with a spherical structure, such as Mode-I. If two or more initiation points are used, the collisions and convergences of these detonation
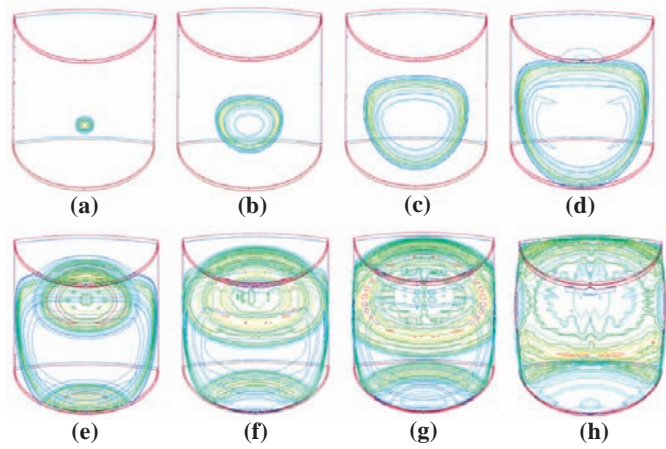
Figure 4. Detonation wave propagation of Mode-I at (a) t = 1.5 μs; (b) t=6.0 μs; (c) t=10.0 μs; (d) t=14.0 μs; (e) t=16.0 μs; (f) t=19.0 μs; (g) t=19.5 μs; (h) t=22.0 μs.
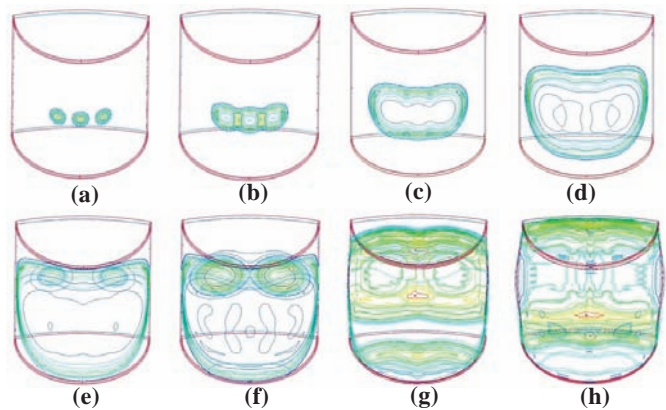
Figure 5. Detonation wave propagation of Mode-II at (a) t = 1.5 μs; (b) t=3.0 μs; (c) t=6.0 μs; (d) t=10.0 μs; (e) t=13.2 μs; (f) t=14.0 μs; (g) t=14.5 μs; (h) t=20.0 μs.
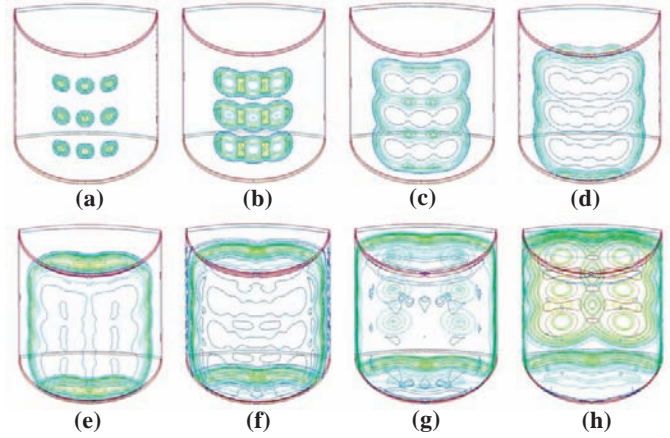
Figure 6. Detonation wave propagation of Mode-III at (a) t = 1.5 μs; (b) t=3.0 μs; (c) t=5.0 μs; (d) t=7.0 μs; (e) t=9.0 μs; (f) t=11.0 μs; (g) t=13.2 μs; (h) t=14.5 μs.
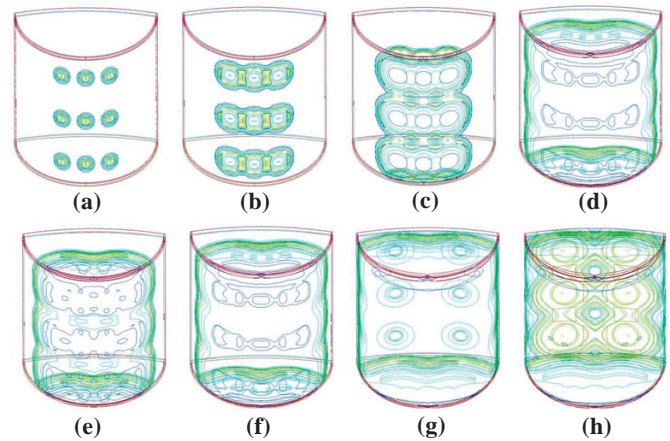
Figure 7. Detonation wave propagation of Mode-IV at (a) t = 1.5 μs; (b) t=3.0 μs; (c) t=4.5 μs; (d) t=7.0 μs; (e) t=9.0 μs; (f) t=11.0 μs; (g) t=13.2 μs; (h) t=14.5 μs.

waves would appear. In Mode-II, three detonation waves form two Mach waves at 3.0 μs and then continue to converge to be one. When Mode-III and Mode-IV are adopted, initial nine detonation waves interact to form six Mach waves at 3.0 μs. Later, six waves continue to propagate, collide, and converge. The wavefront of Mode-I reach the upper shell at 14.0 μs, which delays about 0.8 μs than other three modes. That is because Mach wave has the characteristics of high speed and high pressure. Therefore, the formative bumps of Mach waves reach the upper shell first. Compared with Mode-I and Mode-II, other two modes can obtain relatively good driving wave to fit upper shell well.

Multi-wave interaction is a complicated process in which the wavefront transforms from multiple irregular curved surfaces to a smaller curvature surface after the detonation wave interaction. The curvature of detonation wave has an influence on its stability, and the larger curvature surface is less stable. Flat detonation wavefront can make better driving characteristics[16]. In the case of Mode-III, the axial spacing of initiation points is suitable, and the loading time to upper shell is almost the same. In this condition, the wave curvature of Mode-III is small and stable, and better driven capability can be expected.

4.2 Characteristics of Pressure Distribution

The pressure distribution and wavefront profile are compared for four initiation modes, which are shown in Fig. 8.

When detonation wave reaches the upper shell and the case, the blast compression wave expands outwards, whereas rarefaction wave moves inwards. Expansion waves penetrate into the reaction zone and attenuate detonation wave pressure. Influenced by rarefaction wave, wavefront pressure close to upper shell is 23 GPa, which is 8 per cent lower than the detonation CJ pressure. Multi-point initiation modes have some obvious pressure augment zones where collision and convergence of multi waves occur. The maximum pressure is up to 29 GPa, which increases by 26 per cent. Moreover, it can be seen clearly that wavefront pressure of the side is lower than that of the centre.

From four wavefront profiles, the most match-up wave shape is produced by Mode-III. Enough initiation points and adequate arrangement are all indispensible. It can be predicted that the fragments would be ejected in a more focused way by the match-up wave.
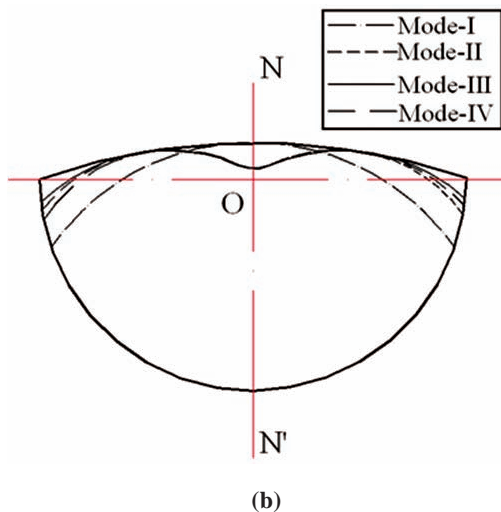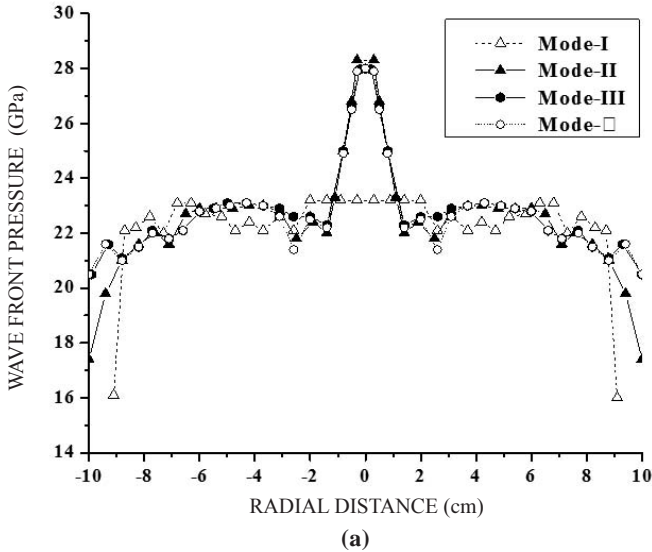
Figure 8. Pressure distribution curve and profile of wave front: (a) pressure distribution curve, and (b) wave front profile.

4.3 Characteristics of Fragment Ejection

When explosive is initiated, the explosive energy is stored inside the case until the explosive pressure exceeds the fracture and yield strength of the case. Before breaking apart, the upper shell will deform firstly to drive outer fragments, thus the fragments obtain high ejection velocity. Fig. 9 shows the ejection results of fragments at 80 μs for four initiation modes.
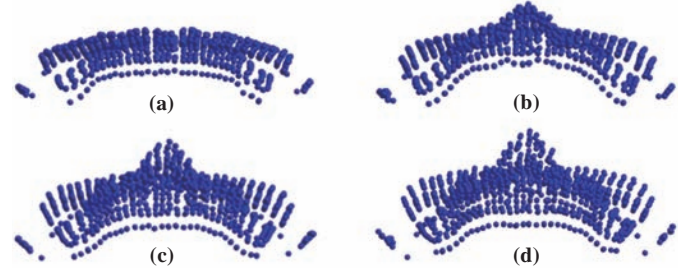
Figure 9. Fragments ejection results of four initiation modes at 80 μs: (a) Mode-I; (b) Mode-II; (c) Mode-III; (d) Mode-IV.

When using single-point mode, distribution is quite uniform around the circumferential direction. The fragments cloud has the same velocity in Mode-I. There are relatively concentrative fragments that are driven in azimuthal direction for other three initiation modes, where the Mach wave increases the detonation pressure. At the same time, the velocity of fragments in the centre is higher.

The proper detonation wave pressure and profile are favourable for fragment spray. To extensively analyze the effect of the detonation wave on fragments, average velocity, distribution density, and total kinetic energy of fragments are calculated. Table 3 shows the ejection results of fragments by different initiation modes.

Table 3. Ejection results of fragments by different initiation modes

Initiation mode	Average velocity (m/s)	Fragment number in 30° (piece)	Distribution density in 30° (pieces/m²)	Total kinetic energy of fragments (kJ)
Mode-I	2046.6	1044	74.0	1956.2
Mode-II	2087.0	1112	78.8	2153.6
Mode-III	2399.6	1154	81.8	2574.8
Mode-IV	2387.6	1106	78.4	2464.3

The average velocity of Mode-III is 2399.6 m/s, which is 1.17, 1.15, and 1.01 times the velocity of Mode-I, Mode-II and Mode-IV, respectively. If the lethal zone angle is 30º, the distribution density of Mode-III is 81.84 pieces/m². In contrast with Mode-III, the distribution density of other three modes decrease by 10.5 per cent, 3.7 per cent, and 4.3 per cent, respectively. That is to say, much more fragments are loaded to spray into the lethal zone if Mode-III is chosen. The larger total kinetic energy in lethal zone is the higher lethality performance could be. The statistical results reveal that the total kinetic energy of fragments of Mode-III is the largest. Compared with Mode-III, the kinetic energies of other modes decrease by 31.6 per cent, 19.6 per cent, and 4.5 per cent, respectively.

4.4 Fragment Distribution

From these analyses, the Mode-III is the optimal initiation mode which has an excellent output property of fragments. The distribution density of fragments by initiation Mode-III is computed, which is displayed in Fig. 10. The comparison of computational data with experimental data shows a good fit.

To interpret these data, a fitted curve is done. The fragment density is given by a Normal distribution of $f(x)$ with respect to ejection angle x, the mathematic model can be expressed as Eqn. (2). Here, the geometric mean $\mu = 0$, standard deviation $\sigma = 10$.

$$f(x) = \frac{1}{10\sqrt{2\pi}} e^{-\frac{x^2}{2\times 10^2}} \tag{2}$$

It can be observed that the distribution density is symmetrical about the N´N which is shown in Fig. 8(b). Moreover, the largest number of fragments appears in the direction of N´N. Within the range of -10° to 10°, the probability of distribution density is close to 70 per cent. If the
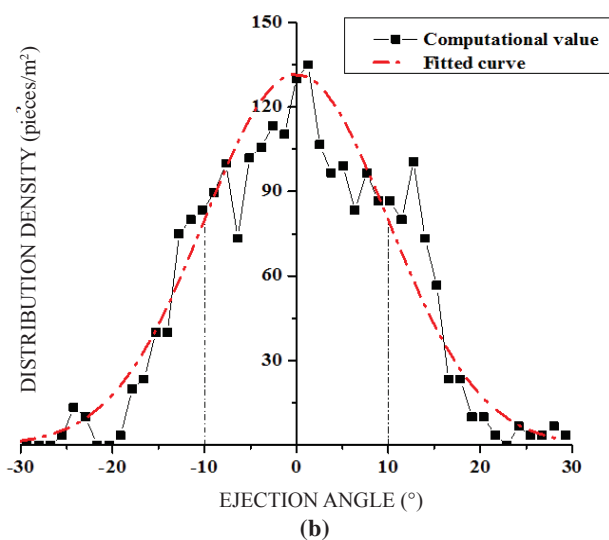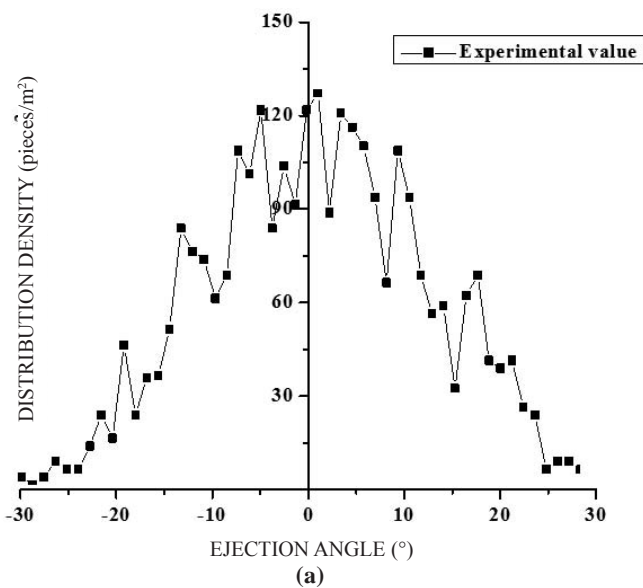
target comes into the ejection angle (-10°, 10°), a large number of effective fragments would be ejected toward the target. It has been proved that the damage efficiency of Mode-III is excellent.

5. CONCLUSION

Three-dimensional simulations were carried out to investigate the detonation wave propagation and detonation output properties for D-shape structure. Detonation wave configuration has great influence on fragment ejection, whereas wave configuration is controlled by initiation mode for a certain structure. Here, four initiation modes are designed to study the detonation wavefront profiles. Spherical wave propagation, collision and convergence are all observed, and pressure distributions of wavefronts are obtained. Simulation results show that three-array-nine-point initiation mode (Mode-III) can produce a match-up wave. Considering output property of detonation, the average velocity, ejection angle, distribution density, and total kinetic energy of Mode-III are all larger than those of other modes. Thus, it can be drawn that Mode-III provides an ideal detonation wave to obtain the largest lethal performance in hitting angle, and the fragment density fits a normal distribution.

REFERENCES

1. Skews, B. & Blitterswijk, A. Shock wave reflection off coupled surface. *Shock Waves*, 2011, **21**, 491-498. doi: 10.1007/s00193-011-0334-y
2. Jimmy, V.; Andrew, J. H. & Robert, A. S. Formation of transverse waves in oblique detonation. *P. Combust. Inst.*, 2013, **34**, 1913-1920. doi: 10.1016/j.proci.2012.07.040
3. Barnat, W. Experimental and numerical study of influence of incidence angle of shock wave created by explosive charge on the steel plate. *Bull. Pol. Ac.: Tech.*, 2014, **62**(1), 151-163. doi: 10.2478/bpasts-2014-0017
4. Kobylkin, I.F. Relation between the critical detonation diameter of explosive charges with characteristics of their shock-wave sensitivity. *Combust. Explo. Shock+*, 2009, **45**(3), 326-330. doi: 10.1007/s10573-009-0043-3
5. Cheval, K.; Loiseau, O. & Vala, V. Laboratory scale tests for the assessment of solid explosive blast effects. *J. Loss Prevent. Proc.*, 2012, **25**, 436-442. doi: 10.1016/j.jlp.2011.11.008
6. Frank, R. & Souers, P. Clark. Corner turning of detonation waves in an HMX-based paste explosive. *Propell. Explos. Pyrot.*, 2000, **25**, 172-178. doi: 10.1002/1521-4087(200009)25:4<172::AID-PREP172>3.3.CO;2-M
7. Williams, D.N.; Bauwens, L. & Oran, E.S. A numerical study of the mechanisms of self-reignition in low-overdrive detonations. *Shock Waves*, 1996, **6**(2), 93-110. doi: 10.1007/BF02515193
8. Teng, H.H.; Zhang, Y.N. & Jiang, Z.L. Numerical investigation on the induction zone structure of the

Figure 10. Distribution density of fragments *vs* ejection angle: (a) experimental data, and (b) computational data.

oblique detonation waves. *Computational Fluids*, 2014, **95**, 127-131. doi: 10.1016/j.compfluid.2014.03.001

9. Zhang, X.F.; Huang, Z.X. & Qiao, L. Detonation wave propagation in double-layer cylindrical high explosive charges. *Propell. Explos. Pyrot.*, 2011, **36**, 210-218. doi: 10.1002/prep.201000004

10. Wei, J.F.; Li, N.; Wen, Y.Q. & Wang, W.J. Initiation style optimization of aimed warhead by numerical simulation. *J. Beijing Inst. Tech.*, 2008, **17**(3), 285-289.

11. Li, W.B.; Wang, X.M. & Li, W.B. The effect of annular multi-point initiation on the formation and penetration of an explosively formed penetrator. *Int. J. Impact Eng.*, 2010, **37**: 414-424. doi: 10.1016/j.ijimpeng.2009.08.008

12. Cao, H.Y.; Chu, E.Y.; Qin, G.S.; Zhou, M.; Liu, T. & Zeng, Z.G. Numerical simulation of overpressure detonation by multi-point array. *Acta Armamentarii*, 2012, **33**, 56-60.

13. Wang, C.; Shu, C.W. & Han, W.H. High resolution WENO simulation of 3D detonation waves. *Combustion Flame*, 2013, **160**(2), 447-462. doi: 10.1016/j.combustflame.2012.10.002

14. Frolov, S. M.; Dubrovskii, A. V. & Ivanov, V. S. Three-dimensional numerical simulation of the operation of the rotating-detonation chamber. *Russ. J. Phys. Chem. B+*, 2012, **6**(2), 276-288. doi: 10.1134/s1990793112010071

15. LSTC. Ls-dyna keyword user's manual (Version 971). Livermore Software Technology Corporation, California, 2007.

16. Watt, S.D. & Sharpe, G.J. Linear and nonlinear dynamics of cylindrically and spherically expanding detonation waves. *J. Fluid Mech.*, 2005, **522**, 329-356. doi: 10.1017/S0022112004001946

CONTRIBUTORS

Dr Ji-Feng Wei, PhD, is presently working as an Associate Professor in the School of Mechatronical Engineering at Beijing Institute of Technology, Beijing, China. He teaches impact mechanics and structural design. His research interests include: explosion mechanics, FE Analysis and impact mechanics.

Mr Chao Zhang is currently a PhD student at the Beijing Institute of Technology, China. His current research interests include: detonation theory and technology, high-speed penetration and collision, shaped charge, and numerical simulation technology.

Dr Shu-Shan Wang, PhD, is currently a Professor in the School of Mechatronical Engineering at Beijing Institute of Technology, China. He teaches terminal effect and structural design. His research interests include: explosion mechanics, impact mechanics and terminal damage effect.